

Supplementary Information for

VSMC-specific EP4 deletion exacerbates angiotensin II-induced aortic dissection by increasing vascular inflammation and blood pressure

Hu Xu^{1*}, Shengnan Du^{2*}, Bingying Fang^{1*}, Chaojie Li^{1*}, Xiao Jia³, Senfeng Zheng¹, Sailun Wang¹, Qingwei Li¹, Wen Su^{4,5}, Nanping Wang¹, Feng Zheng¹, Lihong Chen¹, Xiaoyan Zhang^{1#}, Jan-Ake Gustafsson^{5,6,#} and Youfei Guan^{1#}

¹Advanced Institute for Medical Sciences, Dalian Medical University, Dalian 11644, China.

²Department of Pharmacology, School of Basic Medical Sciences, Zhengzhou University, 100 Science Avenue, Zhengzhou 450001, China.

³Biobank, Peking University Third Hospital, Beijing 100191, China.

⁴Shenzhen University Medical Center, Department of Pathology, Shenzhen 518060, China.

⁵Center for Nuclear Receptors and Cell Signaling, University of Houston, 3013 Cullen Blv, 77204 Houston, Texas, USA.

⁶Center for Innovative Medicine, Department of Biochemistry and Nutrition, Karolinska Institutet, Huddinge, Sweden

* These authors contributed equally to this work.

Corresponding Authors: Prof. Xiaoyan Zhang (wserien@163.com), Jan-Ake Gustafsson (jgustafs@central.uh.edu), or Youfei Guan (guanyf@dmu.edu.cn)

This PDF file includes:

Supplementary text;
Figs. S1 to S10;
Tables S1;
References for SI reference citations

Supplemental Materials and Methods

AngII-infused hypertensive model and ultrasound imaging

Mice were treated with AngII dissolved in sterile saline at 1 µg per kg body weight (µg/kg) per minute using subcutaneous osmotic minipumps (Alzet Corp). After surgery, systolic blood pressure was recorded via the tail-cuff method as previously described (1), and sacrificed on the 28th day after surgery for further experiments.

For in vivo ultrasound images, the aortic diameter was monitored in isoflurane-anesthetized mice (2% isoflurane) by high-frequency ultrasound with a VEVO 3100 echography device (VisualSonics, Toronto, Canada) with 30-µm resolution. Maximal internal diameters of aortic images were measured using VEVO 3100 software (version 1.5.0). All recordings were made by a cardiologist and a technician who were blinded to animal genotype and treatment.

Chemicals and Reagents

Primary antibodies against EP4 and Elf5 in the present study were purchased from Santa Cruz Biotechnology. MMP2, MMP9 and NOX1 antibodies were obtained from Abcam. α -SMA, SM22 α , SMMHC antibodies were from Proteintech. The EP4 agonists prostaglandin E1 alcohol (PGE1-OH) and CAY10580 and antagonists L161,982 and MF498 were purchased from Cayman.

Histology

After euthanization by CO₂ inhalation, mouse aortas were perfused with saline. Aortas were then isolated and fixed in 4% formalin overnight at 4 °C. Paraffin cross-sections (4µm) from organs were stained with hematoxylin and eosin, EVG staining, Masson staining, and Sirius Red staining. Sections were also used for immunohistochemistry or immunofluorescence. Briefly, deparaffinized sections were rehydrated, boiled to retrieve antigens (10 mM citrate buffer, pH 6) and blocked for 45 min with 5% BSA in PBS. Samples were incubated with the following antibodies and reagents for immunohistochemistry or immunofluorescence: mouse anti- α -SMA, mouse anti- SM22 α ,

mouse-anti-SMMHC, rabbit anti-EP4, rabbit anti-F4/80 and dihydroethidium (DHE). Specificity was determined by substituting primary antibody with unrelated IgG (Santa Cruz). For immunohistochemistry, color was developed with DAB, and sections were stained with hematoxylin. For immunofluorescence, secondary antibodies were Alexa-Fluor-633-conjugated goat anti-rabbit antibodies. Sections were mounted with DAPI.

Primary culture of VSMCs

Mouse VSMCs were isolated from 8-12 weeks old EP4 flox/flox mice as described (2), and the cells at passages 3 to 7 were used in experiments. Rat VSMCs were isolated from the thoracic aortic arteries of Sprague-Dawley rats (150-180 g) as described previously (3). The purity of VSMCs was verified by anti-smooth muscle-actin antibody staining, and cells at passages 1 to 6 were used in all experiments.

Western blot and real-time PCR

Western blot was performed as described previously (4). Briefly, proteins from tissues or cells were extracted and quantified. Aliquots of 50 μg total protein or 10 μg membrane protein of each sample were separated by SDS-PAGE and transferred to nitrocellulose membrane. The membrane was blocked at room temperature for 1 h in TBS-T (Tris-buffered saline containing 0.1% Tween 20) containing 5% skimmed milk and was then incubated with primary antibodies at 4°C overnight. The membrane was washed for 5 min with TBS-T buffer for 3-5 times and then incubated with a horseradish peroxidase-conjugated secondary antibody at a dilution 1:5,000 at room temperature for 1 h. After washing, the membrane was developed with ECL Reagent (Vigorous Biotechnology, Beijing) and exposed to Kodak XBT-1 film. The density of the signals was quantified with Image J (NIH) software.

Real-time PCR was performed as described previously (4). Briefly, total RNA was extracted, quantified, and reverse transcribed to cDNA. SYBR Green (Invitrogen, CA) was used as fluorochrome according to the manufacturer's instructions. Primers were designed from the known sequences of mouse genes listed in SI Appendix, Table S1. β -actin was used as an internal standard. The PCR reactions were 94°C for 5 min, and then 35 cycles

of 94°C for 30 s, 59°C for 30 s, and 72°C for 30 s, followed by extension at 72°C for 5 min. Target gene mRNA level was normalized to that of β -actin in the same sample using the 2- Δ Ct method. Each sample was measured in triplicate in each experiment. Moreover, melting curves for each PCR product were analyzed to ensure the specificity of the amplification product.

Blood pressure Measurement

Male mice aged 6-8 months and with 28-33g body weight were used. Following a 2-week training period, blood pressure of mice at the basal level or fed with 7-day high salt diet was measured in conscious EP4^{f/f} and VSMC-EP4^{-/-} mice using the tail-cuff method as previously reported (1) . EP4^{f/f} and VSMC-EP4^{-/-} mice were also used in chronic AngII infusion experiments. For acute infusion studies, mice were anesthetized with 80mg/kg ketamine and 8mg/kg inactin i.p. and placed on a temperature controlled pad. After tracheostomy, PE-10 tubing was inserted into the right carotid artery, and blood pressure was measured with a Cobe CDX II transducer connected to a blood pressure analyzer (BPA 400; Micromed, Louisville, KY) as previously reported (5).

Vascular Tension Assay of Mesenteric Arteries

Mesenteric arteries were isolated from male EP4^{f/f} and VSMC-EP4^{-/-} mice after anesthetized with chloral hydrate (10%) i.p. and cut into rings of 1.0-1.3 mm long in ice-cold modified Krebs-Ringer bicarbonate buffer as previously reported (6). Each segment was suspended between two tungsten wires in chambers of a Multi Myograph System (610M, Danish Myo Technology A/S, Aarhus N, Denmark) for the measurement of isometric force. Each organ chamber was filled with 5ml of the modified Krebs-Ringer bicarbonate solution maintained at 37±0.5 °C and aerated with 95% O₂-5% CO₂ (pH = 7.4). At the beginning of the experiment, each vessel ring was stretched to its optimal resting tension of 1mN for 30 minutes by step-wise stretching and contracted with 60mM KCl to test its contractility. Vessels were brought to their optimal resting tension, equilibrated for 30 minutes and a dose-response to AngII in vessels was determined after pretreating with L-NAME (0.1mM). A dose-response to phenylephrine in vessels was also determined after pretreating with/without L-NAME (0.1mM). To eliminate the

vasodilation responses of mesenteric resistance arteries, a dose-response to acetylcholine was determined.

Ca²⁺ Imaging in Cultured VSMCs

Rat and mouse VSMCs were loaded with the Ca²⁺ indicator fluo-4 AM (2.5 μmol/L, Molecular Probes) in Tyrode's solution for 10 minutes in the dark at 37°C. After washed to remove excess indicator, cells were imaged in Ca²⁺ free Tyrode's solution at 23°C using a Leica SP8 Live inverted confocal microscope (Leica, Germany) equipped with a 40x oil immersion objective, at 90 frames/min, with the excitation laser at 488 nm and 505-530 nm emission as previously reported (6) .

Statistical analysis.

Data are presented as mean±SEM. Statistical analyses were performed using GraphPad Prism 5 software. Comparisons between 2 groups were analyzed by Student's t test except the time-course studies in the two genotypes. Comparison among groups in the time-course studies was made by repeated-measures ANOVA using SAS. p<0.05 was considered statistically significant.

Supplemental Figures and tables

Figure S1

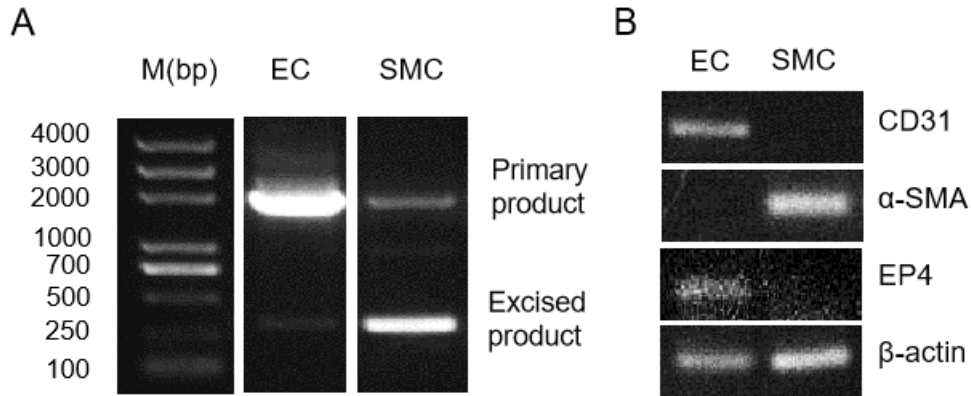


Figure S1. Validation of EP4 deficiency in VSMCs.

A. PCR analysis showing sufficient deletion of the exon 2 of EP4 gene in the aortic smooth muscle layer in VSMC-EP4^{-/-} mouse. Little deletion of EP4 gene was evident in aortic endothelium layer. EC: endothelial cell; SMC: smooth muscle cell.

B. RT-PCR assay demonstrating the absence of EP4 mRNA in the aortic smooth muscle layer of VSMC-EP4^{-/-} mouse.

Figure S2

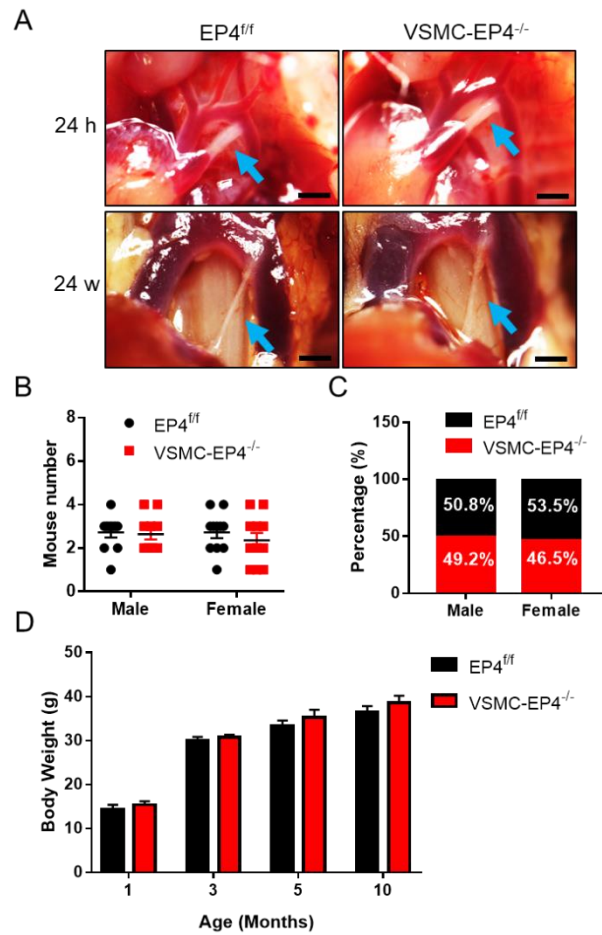


Figure S2. VSMC-specific deletion of EP4 does not affect the closure of the ductus arteriosus, the survival and growth of mice.

A. Photographic figures showing the ductus arteriosus of neonatal (24 hours after birth) and adult (24 weeks old) EP4^{f/f} and VSMC-EP4^{-/-} mice.

B. Gender difference in mice with EP4^{f/f} and VSMC-EP4^{-/-} genotypes. EP4^{f/f} mice were crossed with SMMHC_Cre⁺ mice. Male and female offsprings with different genotypes were counted.

C. Genotypic difference in both male and female mice. The percentage of cre-positive (VSMC-EP4^{-/-}) and cre-negative (EP4^{f/f}) mice were calculated.

D. Body weight of male EP4^{f/f} and VSMC-EP4^{-/-} mice with different ages.

Figure S3

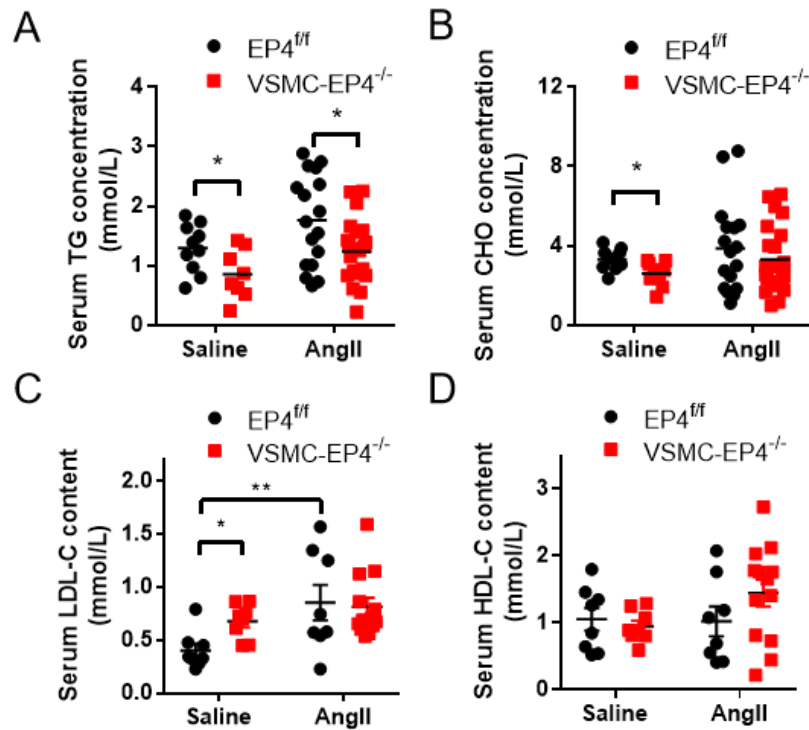


Figure S3. Effect of AngII infusion on serum lipid profile in WT and VSMC- $EP4^{-/-}$ mice.

A&B. Total serum triglycerides (TG) and cholesterol (Ch) concentrations in WT ($EP4^{f/f}$) and VSMC- $EP4^{-/-}$ mice following saline or AngII infusion for 28 days. $n=8-22$, $*p<0.05$.

C&D. Serum LDL-Ch and HDL-Ch levels of saline- or AngII-infused $EP4^{f/f}$ and VSMC- $EP4^{-/-}$ mice. $n=8-13$, $*p<0.05$, $**p<0.01$.

Figure S4

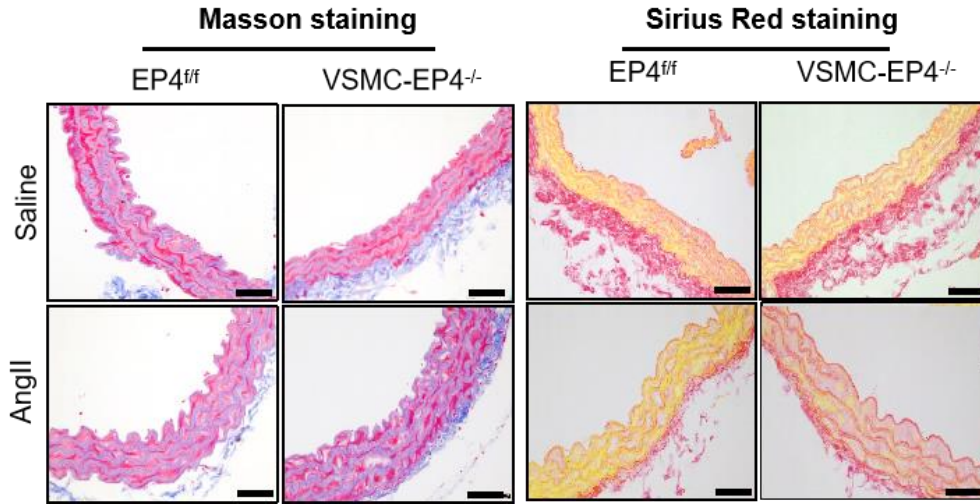


Figure S4. No difference in aortic collagen content between EP4^{f/f} and VSMC-EP4^{-/-} mice.

Representative staining of collagen in saline- and AngII-treated mice as assessed by the Masson and Sirius Red stains. Scale bars: 100 μ m.

Figure S5

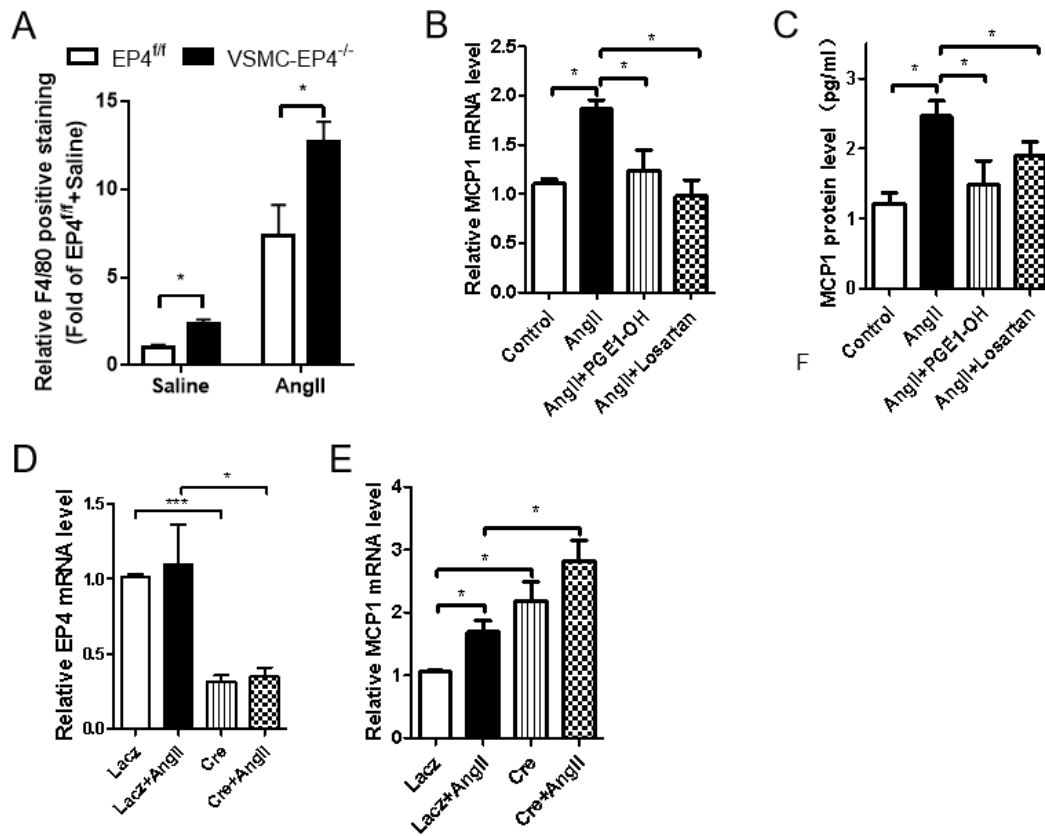


Figure S5. EP4 suppresses MCP-1 expression in cultured VSMCs.

A. Semi-quantitative analysis of aortic F4/80 expression in Figure 4B. n=3-4, *p<0.05.

B&C. Real-time PCR analysis (A) and enzyme-linked immunosorbent assay (ELISA) (B) of MCP-1 mRNA expression and protein secretion. Cultured wild-type VSMCs were pretreated with the EP4 agonist PGE1-OH (100 nM) or the AT1 antagonist losartan (1µM) for 2 hours, followed by AngII (100 nM) treatment for 24 hours. n=3, *p<0.05.

D&E. EP4 mRNA expression (C) and MCP-1 mRNA expression (D) in EP4^{fl/fl} VSMCs infected with Cre adenovirus or Lacz adenovirus for 48 hours. n=3, *p<0.05.

Figure S6

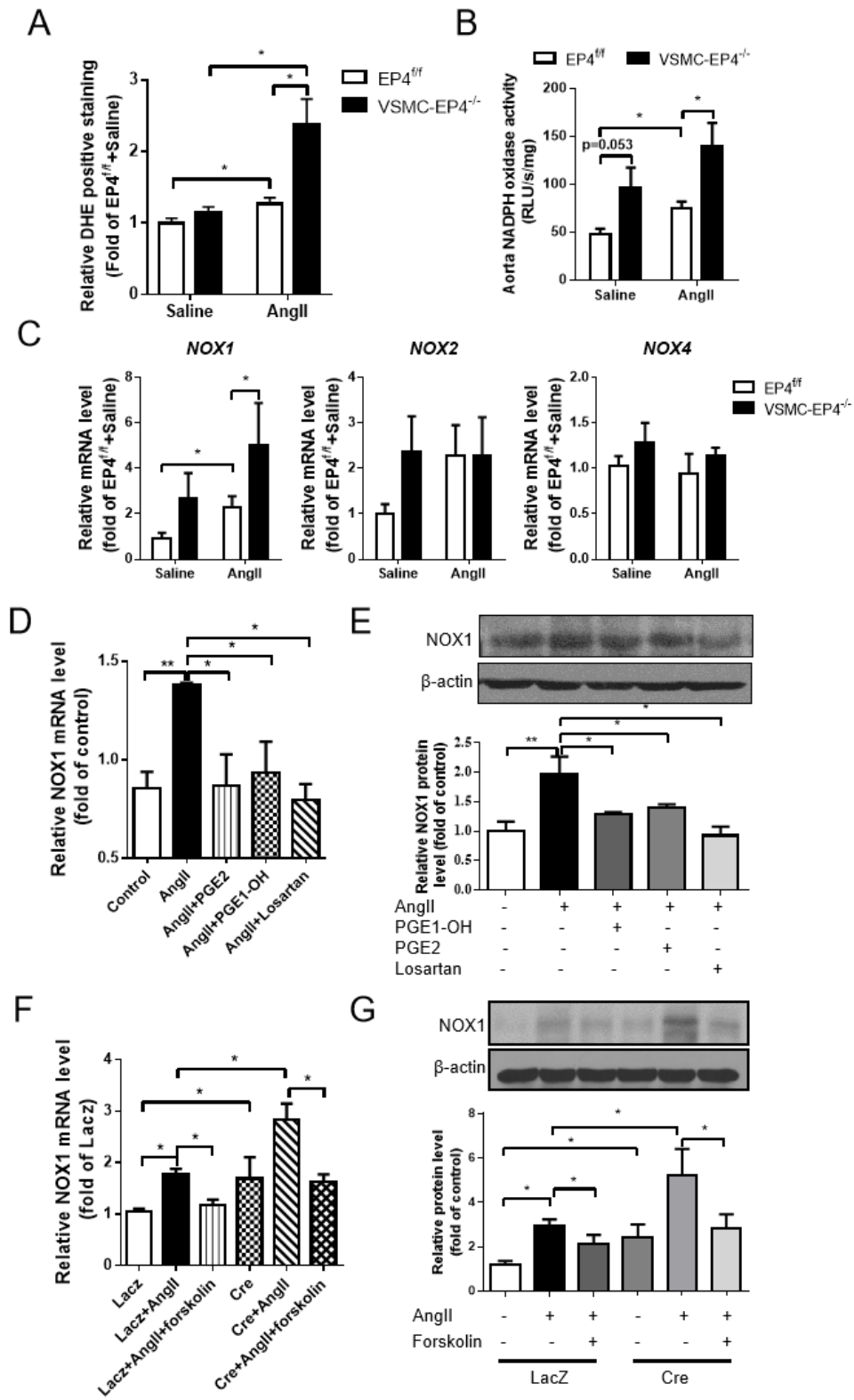


Figure S6. EP4 suppresses NOX activity in mice and NOX1 expression in cultured VSMCs.

A. Semi-quantitative analysis of aortic superoxide anion levels in Figure 4C. n=3-4, *p<0.05.

B. Lucigenin chemiluminescence analysis for aortic NADPH oxidase activity in each treatment group. n=3, *p<0.05.

C. Real-time PCR analysis of mRNA levels of NOX1, NOX2 and NOX4 in the aortas of AngII-infused mice. n=7-9, *p<0.05.

D&E. Quantitative PCR (G) and Western blot (H) analysis of NOX1 expression in VSMCs treated with AngII (100nM) with or without PGE2 (1 μ M), PGE1-OH (100 nM) and losartan (1 μ M). n=3, *p<0.05, **p<0.01.

F&G. mRNA (I) and protein (J) expression of NOX1 in EP4^{f/f} VSMCs infected with Cre adenovirus or LacZ adenovirus in the presence of AngII (100 nM) with or without forskolin (1 μ M). n=4, *p<0.05.

Figure S7

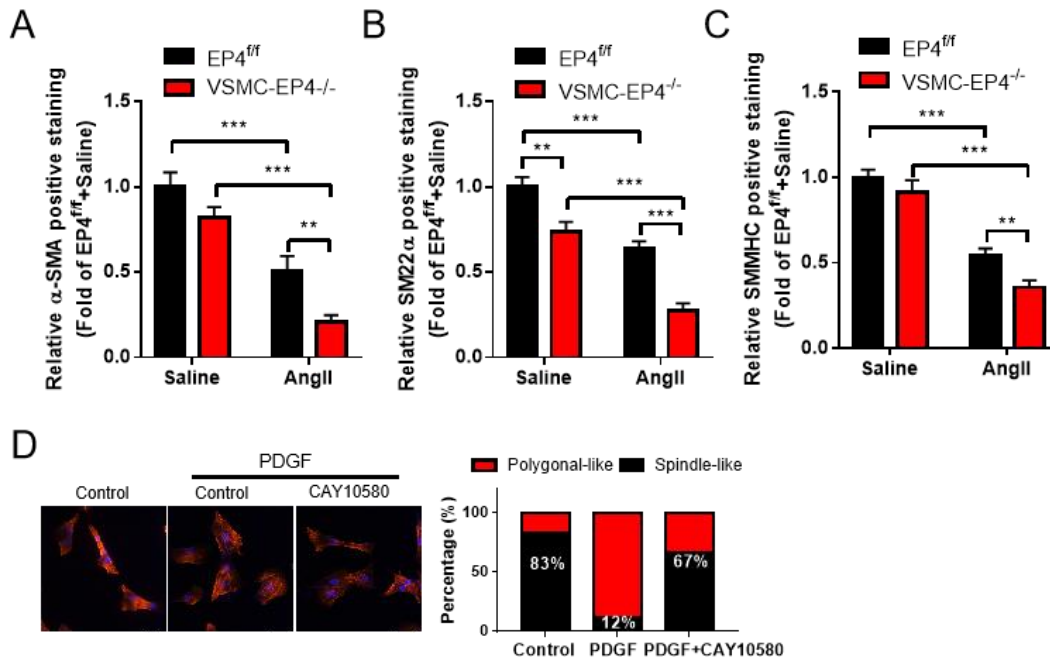


Figure S7. EP4 is essential for maintaining VSMC contractile phenotype.

A-C. Semi-quantitative analysis of α -SMA (A), SM22 α (B) and SMMHC (C) in Figure 5A-C. n=7-14, **p<0.01, ***p<0.001.

D. Representative images of F-actin (red) distribution of the EP4 agonist CAY10580 (100 nM)-treated aortic VSMCs in the presence of PDGF-BB (25 ng/ml). DAPI staining was used to stain the nuclei (blue). The values were expressed as a percentage of spindle-like or polygonal-like cells.

Figure S8

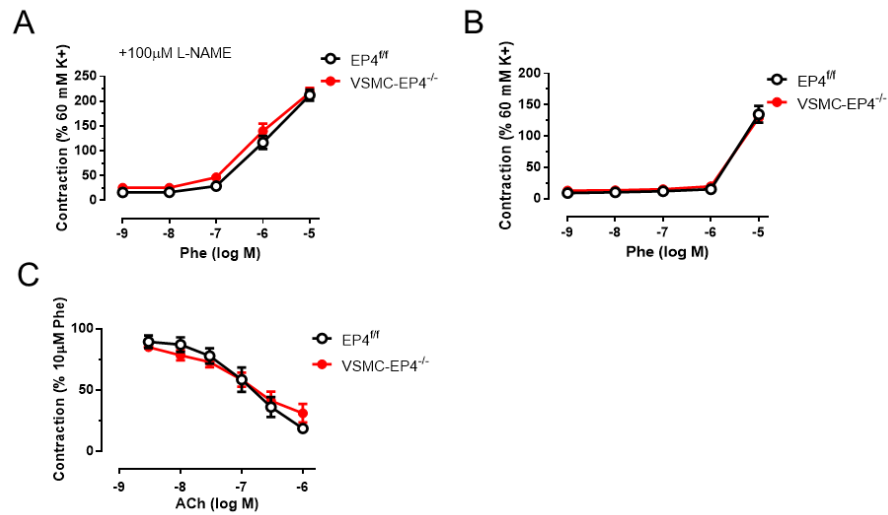


Figure S8. No difference in phenylephrine (Phe)-evoked vasoconstriction and acetylcholine (ACh)-induced vasodilatation between EP4^{f/f} and VSMC-EP4^{-/-} mice.

A&B. Phenylephrine (Phe)-evoked vasoconstriction of mesenteric arterial rings from EP4^{f/f} and VSMC-EP4^{-/-} mice. The rings were pretreated with or without L-NAME (100 μM) and then challenged with various doses of Phe. No difference was found between two genotypes, n=5-10.

C. Acetylcholine (ACh)-induced vasodilation responses of mesenteric arteries from EP4^{f/f} and VSMC-EP4^{-/-} mice. No difference was found between two genotypes, n=6.

Figure S9

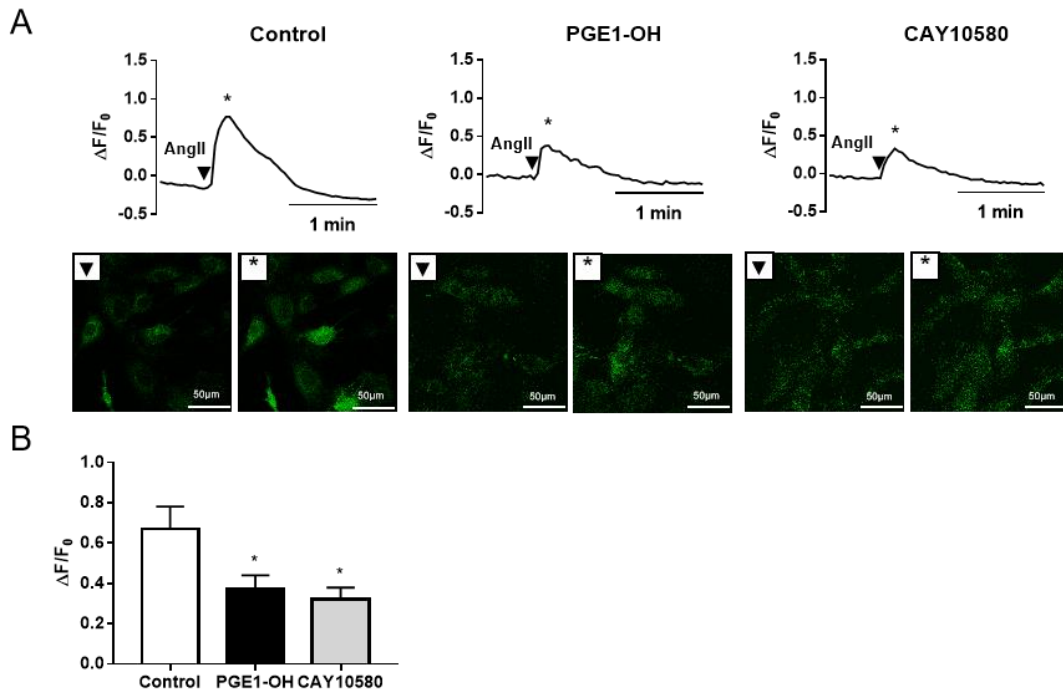


Figure S9. Activation of EP4 suppresses AngII-induced increase in intracellular Ca^{2+} levels.

A. Representative images of AngII-induced intracellular Ca^{2+} spark in VSMCs by the EP4 agonists. VSMCs were pre-incubated with the EP4 agonist PGE1-OH or CAY10580 for 30 minutes. \blacktriangledown represents Ca^{2+} fluorescence images at baseline. * indicates images at the peak of induction.

B. Ratio of peak-to-basal change ($\Delta F/F_0$) in Fluo-4 AM fluorescence intensity in VSMCs treated with PGE1-OH or CAY10580. $n=5-8$, $*p < 0.05$ vs. control.

Figure S10

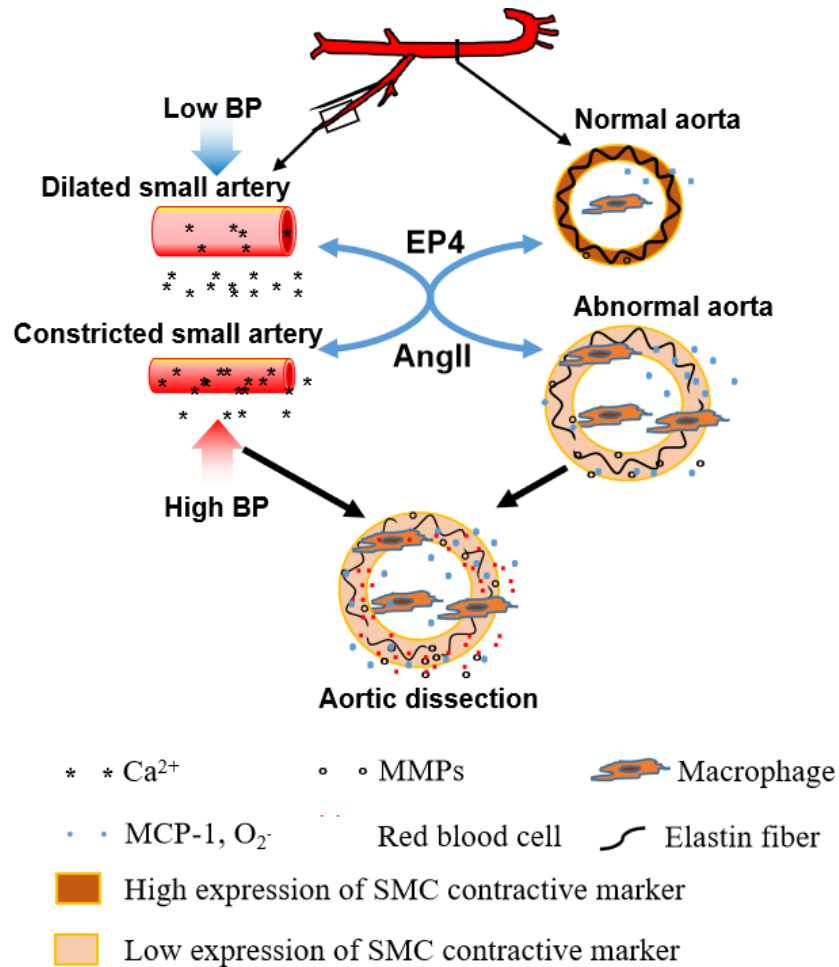


Figure S10. Graphic illustration of the effect of VSMC-specific EP4 deficiency on aortic dissection.

EP4 attenuates AngII-induced small artery vasoconstriction and hypertension via reducing intracellular Ca^{2+} concentration in VSMCs. VSMC-specific EP4 deletion sensitizes mice to AngII-induced hypertension and enhances AngII-elicited vascular inflammation, smooth muscle cell dedifferentiation, oxidative stress and MMP2/9 activity, leading to the occurrence of aortic dissection.

Table S1. Primer pairs used for amplifying mouse genes.

Gene Name	Forward primer sequence (5'-3')	Reverse primer sequence (5'-3')
EP4	ATGGTCATCTTACTCATCGCCAC	CCTTCACCACGTTTGGCTGAT
NOX1	ACAACAGCACTCACCAATGC	TTTTGAGCTTGTTGTCGGCA
NOX2	TTTGTCAAGTGCCCAAGGT	GGCATCTTGGAACCTCTGCT
NOX4	TGTGCCTTTATTGTGCGGAG	GCTGATACTGGGGCAATG
MCP1	AATGAGTAGCAGCAGGTGAGTG	GAAGCCAGCTCTCTTTCCTC
MMP2	GCACATCCTATGACAGCTGC	TTTGTTGCCCAGGAAAGTGA
MMP9	GAGACTCTACACCCAGGACG	GAAAGTGAAGGGGAAGACGC
EP1	TAACGATGGTCACGCGATGG	ATGCAGTAGTGGGCTTAGGG
EP2	ATGCTCCTGCTGCTTATCGT	AGGGCCTCTTAGGCTACTGC
EP3	GGATCATGTGTGTGCTGTCC	GCAGAACTTCCGAAGAAGGA
β -actin	CCCTGGAGAAGAGCTACGAG	CGTACAGGTCTTTGCGGATG

Reaction temperature was 59°C for all genes.

Supplementary References

1. Krege JH, Hodgin JB, Hagaman JR, & Smithies O (1995) A noninvasive computerized tail-cuff system for measuring blood pressure in mice. *Hypertension (Dallas, Tex. : 1979)* 25(5):1111-1115.
2. Zhao G, *et al.* (2017) Unspliced XBP1 Confers VSMC Homeostasis and Prevents Aortic Aneurysm Formation via FoxO4 Interaction. *Circulation research* 121(12):1331-1345.
3. Jovinge S, Hultgardh-Nilsson A, Regnstrom J, & Nilsson J (1997) Tumor necrosis factor-alpha activates smooth muscle cell migration in culture and is expressed in the balloon-injured rat aorta. *Arteriosclerosis, thrombosis, and vascular biology* 17(3):490-497.
4. Xu H, *et al.* (2016) Prostaglandin E2 receptor EP3 regulates both adipogenesis and lipolysis in mouse white adipose tissue. *Journal of molecular cell biology* 8(6):518-529.
5. Wang JF, Hampton TG, Deangelis J, Travers K, & Morgan JP (1999) Differential depressant effects of general anesthetics on the cardiovascular response to cocaine in mice. *Proceedings of the Society for Experimental Biology and Medicine. Society for Experimental Biology and Medicine (New York, N.Y.)* 221(3):253-259.
6. Wang X, *et al.* (2015) Nuciferine relaxes rat mesenteric arteries through endothelium-dependent and -independent mechanisms. *British journal of pharmacology* 172(23):5609-5618.